

## First steps in the spreading of a liquid droplet

Anne-Laure Bianco, Christophe Clanet,\* and David Quéré

Laboratoire de Physique de la Matière Condensée, UMR 7125 du CNRS, Collège de France, 75231 Paris Cedex 05, France

(Received 14 March 2003; published 14 January 2004)

We describe the first steps of spreading of a liquid droplet brought in contact with a solid that it wets completely. Usually, it is assumed that the dynamics of the droplet results from a balance between the spreading forces and viscosity. But before this classical stage, inertia resists to the motion, which leads to a very different dynamic law. We study experimentally the nature of this law, compare our results with recent theoretical predictions, and determine the duration of this inertial regime.

DOI: 10.1103/PhysRevE.69.016301

PACS number(s): 47.55.Dz, 68.05.-n

The dynamics of a droplet spreading on a solid in a situation of complete wetting has been studied quite extensively for the past 20 years [1–7]. The main findings can be summarized as follows: a microscopic precursor film propagates ahead of the macroscopic drop, which spreads on a solid wetted by this precursor [5,6]. The drop is first drawn by the gradient of curvature (and thus of Laplace pressure) between its periphery and its center; later, when it becomes centimetric in size, gravity becomes the dominant spreading force. Both the driving forces are quite weak, and become weaker as time goes on, which leads to a strong reduction of the drop velocity as a function of time  $t$ . Balancing these forces with the viscous friction successively yields an increase of the drop radius as  $t^{1/10}$  (in the first capillary stage) [3–7], and as  $t^{1/8}$  (in the next gravitational regime) [1,2]. In the first steps of the spreading, these laws predict a divergence of the velocity, in contradiction with the assumption of a viscous flow, and should not be valid any longer. Here, we investigate how a drop behaves just after being brought in contact with a substrate that it wets totally.

The key point is to achieve a device allowing us to make a spherical droplet approach a solid surface with a negligible speed: releasing a drop out of a pipette from a height as low as 2 mm makes it impact the solid at  $20 \text{ cm s}^{-1}$  a velocity for which the inertia of the moving drop dominates the first steps of spreading. (In addition, such a drop vibrates just after it detached, which also complicates the analysis.)

In our experiment, we first deposit a drop (mostly pure water, of viscosity  $\eta = 1 \text{ mPa s}$ ) on a superhydrophobic substrate. On such a material, the contact angle is of the order of  $160^\circ$ – $170^\circ$ , and the adhesion is highly reduced [8]. For drops smaller than the capillary length  $a \equiv \sqrt{\gamma/(\rho g)}$  (denoting the surface tension and density of the liquid as  $\gamma$  and  $\rho$ ), that is, millimetric or less, the drop is quasispherical since surface forces then dominate gravity. Practically, the radius  $R$  of the drops was between 0.5 mm and 3 mm.

Then, a solid which is totally wet by water is brought in contact with the drop, from above (Fig. 1). Glass plates were chosen for this purpose, and exposed to a flame before each experiment. This treatment clears them of their contami-

nants, and makes them wettable for at least 5 min, that is, much longer than the duration of each experiment. The plate is slowly lowered, thanks to a micrometric screw (at a velocity that we checked using a camera to be smaller than  $0.5 \text{ mm s}^{-1}$ ), till it contacts the drop. Side or top views of the spreading were performed using an ultrafast camera (9000 frames per sec.).

We display in Fig. 2 a sequence of snapshots corresponding to the early stage of the spreading of a water drop of volume  $5 \mu\text{l}$  ( $R = 1 \text{ mm}$ ). Time increases from left to right with intervals of 1.1 ms between each image.

The propagation of the solid/liquid contact (of radius  $r$ ) is observed to be extremely fast: the drop immediately loses its spherical shape. A region of high curvature appears close to the contact, and a capillary wave propagates from the top to the bottom of the drop. The end of the spreading is not shown here: the bottom of the drop detaches from the superhydrophobic substrate, and the spreading continues on the glass plate, till gravity balances capillary forces (which implies a centimetric contact with the solid, much larger than the size of each snapshot in Fig. 2).

Figure 3 shows examples of the temporal evolution of this contact, corresponding to three different drop sizes. The data are presented in a log-log plot, and our main result is a common behavior for the different experiments: in each case, the contact radius is observed to increase as the square root of time, before slowing down. The time  $\tau$ , which defines the duration of this first regime of spreading, increases with the size of the drop. The second regime of spreading ( $t > \tau$ ) can

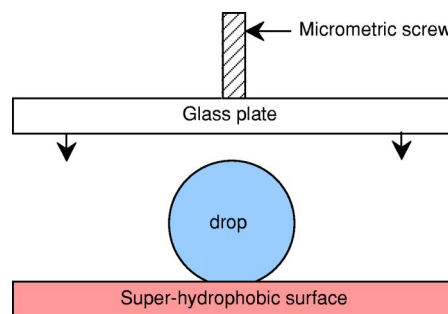


FIG. 1. Side view of our experimental setup: a drop, which is deposited on a superhydrophobic solid, is slowly approached and contacted by a very clean plate of glass, both smooth and wettable.

\*Institut de Recherche sur les Phénomènes Hors Équilibre, UMR 6594 du CNRS, Boîte Postale 146, 13384 Marseille Cedex, France.

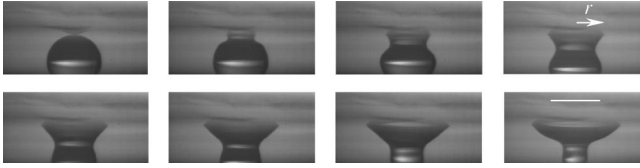


FIG. 2. Water droplet of volume  $5 \mu\text{l}$  spreading on a surface of glass (we denote the water/glass contact as  $r$ ). The time interval between two successive images is 1.11 ms and the bar in the last picture indicates 2 mm.

also be characterized by an exponent ( $r \sim t^\alpha$ ), and  $\alpha$  is found to be of the order of 0.1, the classical value resulting from a balance between viscosity and capillarity [5–7].

A scaling law was recently proposed by Eggers, Lister, and Stone to describe the first stage of coalescence of two liquid drops of small viscosity, taking into account the dominant role of inertia in this regime [9]. This model was recently confirmed in numerical simulations by Duchemin *et al.*, in the same limit of inviscid liquids [10]. Here we propose to adapt these arguments to the case of a drop spreading on a solid. At short time, the curvature  $\kappa$  of the interface which drives the liquid is related to the lengths  $r$  and  $R$  by the geometrical relation:

$$\kappa \sim \frac{R}{r^2}.$$

The gradient of this curvature induces a gradient of Laplace pressure  $f$ , which can be written dimensionally  $f \sim \gamma R/r^3$ , and which is the driving force of the spreading. The mass  $m$  of liquid which is entrained by this force scales as  $\rho r^2/\kappa \sim \rho r^4/R$ , which gives a total force  $F \sim \gamma r$  (logically proportional to the surface tension and to the perimeter of the moving contact). Neglecting the role of viscosity, the equation of the motion reduces to  $dmv/dt = F$  (denoting  $v = dr/dt$  as the velocity), and thus can be written

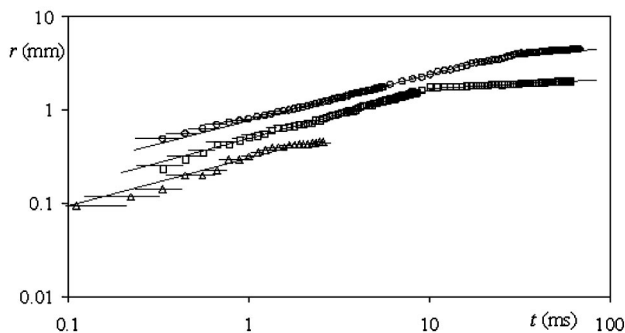


FIG. 3. Radius  $r$  of the solid/liquid contact for a water drop brought in contact with a glass plate that it wets totally.  $r$  is plotted as a function of time in a log-log representation, for three different drop radii:  $R = 1.2 \text{ mm}$  ( $\circ$ ),  $R = 0.7 \text{ mm}$  ( $\square$ ), and  $R = 0.27 \text{ mm}$  ( $\triangle$ ). For each curve, the slopes 1/2 and 1/10 are successively indicated [as suggested by Eqs. (1) and (3)]. The duration  $\tau$  of the first regime is observed to increase with the drop size.

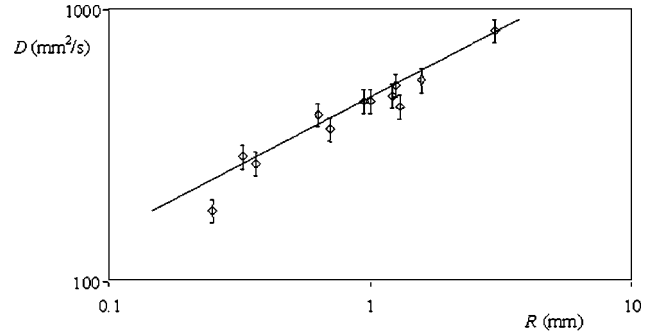


FIG. 4. Dynamic coefficient [defined in Eq. (2)] for the size of the solid/liquid contact in the inertial regime of spreading, as a function of the drop radius. The full line is the best fit, and provides a slope of 0.52.

$$\frac{d}{dt} \left( r^4 \frac{dr}{dt} \right) \sim \frac{\gamma R}{\rho} r.$$

In this equation, both the mass of liquid and the force vary with time a feature which is different from similar problems such as the inertial capillary rise, or the onset of menisci, for which the geometry fixes a constant value for the driving force [11,12]. Hence, the solution which comes out is different. One finds

$$r^2(t) \sim Dt \quad (1)$$

with

$$D = \sqrt{\frac{\gamma R}{\rho}}. \quad (2)$$

This coefficient  $D$  appears as a very natural quantity, it can be expressed as  $R^2/T$ , where  $T \sim \sqrt{\rho R^3/\gamma}$  is the inertial/capillary time scale, a drop of mass  $M \sim \rho R^3$  can be seen as a spring of stiffness  $\gamma$ , and  $T$  is thus the natural response time of this spring (it is for example, the time scale of vibration of a free drop in air) [13].

The size of the solid/liquid contact was indeed observed in Fig. 3 to obey a square-root growth in the first regime, as expected from Eq. (1). But this alone is not enough: a drop impacting on a solid at a speed  $V$  should also generate such a law at short time, for geometric reasons. The depth on which the drop is deformed can be written  $\delta = Vt$ , and the size  $r$  of the contact and  $\delta$  are related by the geometric relation (for  $r \ll R$ )  $r^2 \sim R\delta$ , which eventually yields  $r^2 \sim RVt$ . In our case,  $V$  is less than  $0.5 \text{ mm s}^{-1}$ , which implies an impact coefficient  $RV$  less than  $5 \times 10^{-3} \text{ cm}^2 \text{ s}^{-1}$ , much smaller than the one predicted by Eq. (2) ( $D$  of the order of  $2 \text{ cm}^2 \text{ s}^{-1}$ ). In order to go beyond this simple qualitative fact, we studied the structure of the coefficient  $D$ . Its value was measured using plots such as the one displayed in Fig. 3, and it is reported in Fig. 4 as a function of the size of the drop, in a log-log plot.

The data are found to obey a scaling law, providing as an exponent  $0.52 \pm 0.05$ , in good agreement with Eq. (2). The dimensional numerical prefactor deduced from the experi-

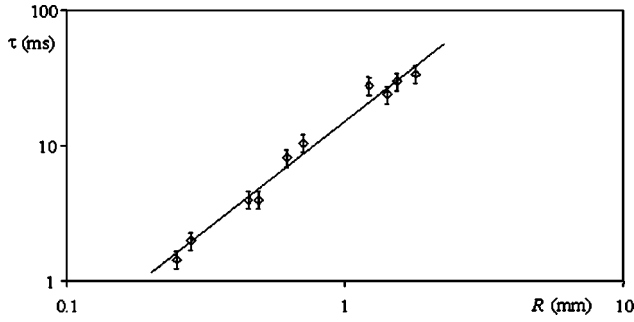


FIG. 5. Duration of the inertial regime [described by Eqs. (1) and (2), and observed in Fig. 3], as a function of the drop radius. The full line indicates the slope 1.62.

ments is  $17 \times 10^{-3}$ , of the same order of magnitude as  $\sqrt{\gamma/\rho}$  which is about  $8 \times 10^{-3}$  for water.

We finally investigated the duration of the inertial regime. Once the liquid is moving, the factor which limits the dynamics of the spreading is not inertia anymore, but viscosity. Then, the drop is close to a spherical cap joining the solid with a dynamic angle  $\theta$ , whose value is given by Tanner's law,  $\theta^3 \sim \eta V/\gamma$  [3]. Together with the conservation of volume ( $r^3 \theta \sim R^3$ ), this yields the classical law of viscous spreading of a small drop [5]:

$$r(t) \sim R \left( \frac{\gamma t}{\eta R} \right)^{1/10}. \quad (3)$$

Therefore, at short time, inertia is indeed the limiting factor of the spreading: the radius  $r$  given by Eq. (1) is then necessarily smaller than the one given by Eq. (3). But if we wait long enough, the two curves must cross each other, and we fall in the viscous regime. The crossover is given by equating the radii given by Eqs. (1) and (3), which yields as a characteristic time  $\tau$  of duration of the inertial regime,

$$\tau \sim \left( \frac{\rho \gamma R}{\eta^2} \right)^{1/8} \sqrt{\frac{\rho R^3}{\gamma}}, \quad (4)$$

where we chose to isolate the time  $T \sim \sqrt{\rho R^3/\gamma}$  defined above as the inertial/capillary time scale of a drop of radius  $R$ . For a millimetric water drop, the typical duration  $\tau$  which can be evaluated from Eq. (4) is of the order of 1 ms, in good agreement with our experiments in Fig. 3. More quantitatively, we could extract from this plot (and other similar ones) the time  $\tau$ : the transition between the two successive regimes is well-cut, providing an accurate measurement of this time. We report in Fig. 5 the value of  $\tau$  as a function of the drop radius, in a log-log plot.

There again, we note that the data are fairly well described by a scaling law. The exponent is found to be  $1.62 \pm 0.05$ , in very good agreement with Eq. (4), which predicts  $13/8$  for this exponent.

The time  $\tau$  depends very weakly on the parameters characterizing the liquid ( $\eta$ ,  $\gamma$  and  $\rho$ ) and appears to be mainly fixed by the drop size. Using mixtures of water and glycerol, we checked experimentally the dependence in viscosity of  $\tau$ . The results are reported in Fig. 6, showing over three de-

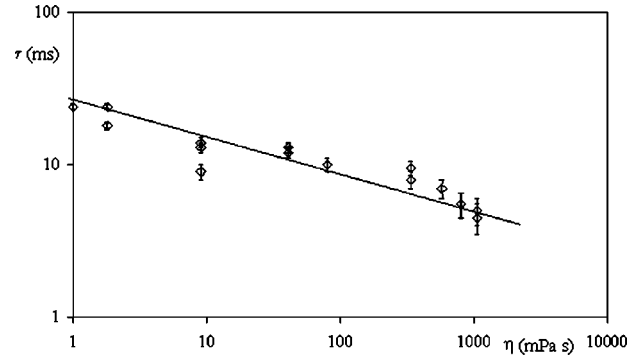


FIG. 6. Duration of the inertial regime [described by Eqs. (1) and (2), and observed in Fig. 3], as a function of the liquid viscosity. The full line indicates the slope  $-1/4$ .

acades of liquid viscosity a slope close to  $-1/4$  (continuous line), in fair agreement with Eq. (4). This weak dependency has an interesting consequence: introducing the duration of the inertial regime in the dynamic law [Eq. (1)], we find that the spatial extension of this regime scales as  $R(\gamma\rho R/\eta^2)^{1/16}$ . This expression is remarkably insensitive to the liquid viscosity, showing that the extension of the inertial regime should be of the order of the drop size, even for quite viscous liquids.

Let us finally conclude by emphasizing different peculiarities of this dynamic system.

(1) At the small scale where surface forces are dominant, the dynamics of interfaces is often dictated by a balance between these forces and viscosity. However, strong deviations towards these classical laws can be observed at short time. This can generally be interpreted by considering inertia, as shown for example in capillary rise [11,12]. We reported here such an inertial regime for a spreading drop. We found that the first steps of the wetting are well described by a square-root growth, instead of the usual very slow behaviors, which set at longer times (mainly fixed by the size of the drop). The duration of this regime is typically of the order of 1 ms for a millimetric water drop which looks short, yet because of a high speed corresponds to quite large extensions (typically about the drop size) of the solid/liquid contact. This inertial regime should thus be relevant in many practical situations, such as soldering, detergency, bridge formation (such as observed using SFA or AFM), or coalescence of liquids of low viscosity.

(2) We can deduce from Eq. (1) the velocity  $V$  with which the center of mass of the drop approaches the plate. Noting  $\delta$  as the lowering of this point, and using the geometrical relation  $\delta \sim r^2/R$ , we find that  $V$  is constant and equal to  $\sqrt{\gamma/(\rho R)}$ . The latter expression expresses a transfer of surface energy in kinetic energy, which is also found in other inertial motions of interfaces, such as capillary rise [12] or coalescence [10]. It also fixes the impact velocity below which the inertial spreading described here will dominate the forced spreading induced by the impact velocity. For small drops ( $R \approx 100 \mu\text{m}$ ), this velocity is high (about  $1 \text{ m s}^{-1}$ ).

(3) The spreading is all the quicker since the drop is large [Figs. 1 and 2, Eq. (2)], a very unusual feature in an inertial process where it is the mass which resists to the motion.

However, the local character of the motion allows us to understand this fact. The mass of moving liquid scales as  $\rho r^2 \delta$ , and thus (for a given  $r$ ) decreases with the drop radius  $R$ , while the rest of the drop (i.e., most of the mass) remains immobile in these first steps of spreading.

(4) The spreading law in this regime [Eq. (1)] does not depend on the so-called spreading parameter, that is, on the nature of the substrate. We checked this point by making the substrate liquid instead of solid. We prewetted a glass plate with a water film of thickness  $200 \mu\text{m}$ , and studied the spreading of a water drop ( $R = 1.4 \text{ mm}$ ) on this film, using the setup sketched in Fig. 1. The law for the liquid/liquid contact was found to obey Eq. (1), giving  $D = 7.5 \times 10^{-4} \text{ m}^2 \text{ s}^{-1}$ , in good agreement with the value expected from Fig. 4 for a drop of this size. The fact that a liquid spreads similarly on a wet and on a dry solid first arises from the presence of a microscopic precursor film in the latter case, which makes the driving force proportional to the sole liquid surface tension [6]. It also stresses the inertial nature of the spreading: a viscocapillary motion would have been much quicker on a prewetted substrate, because of the lubricating effect of this layer.

(5) The inertial stage of the spreading was found to obey the laws predicted by Eggers *et al.* for the coalescence of two inviscid liquid drops [9,10]. This can be understood by the nature of the driving force (as stressed above), which is just fixed by the gradient of curvature of the liquid/vapor interface, but also by a geometry argument: for two coalescing

drops the flow is forced by symmetry in the direction perpendicular to the contact, a common feature with a spreading drop. The experiments reported here thus appear as a first step for understanding quantitatively the dynamics of coalescence between liquids of low viscosity. More generally, three main factors are likely to slow down the motion in both cases: viscous effects in the region of high curvature, the inertia of the droplet, and the viscosity in the whole droplet. (In our particular device (see Fig. 1), we could add gravity, but it can be neglected in the first steps of the spreading.) Each of these factors generate an original spreading law, and we reported here two of them. Eggers *et al.* predicted that the regime dominated by viscous effects in the cusp region only concerns very small lengths, that is, extremely short time [9], which are not investigated here. In order to compare the effects of inertia and viscosity, we can build the ratio between an inertial velocity and a viscous one. The former can be defined as  $R/T$ , and the latter as  $\gamma/\eta$ , which finally gives for their ratio:  $\text{Oh} \equiv \eta/\sqrt{\gamma\rho R}$ . This dimensionless number is often referred to as the Ohnesorge number, and discriminates in most cases inertial regimes from viscous ones [9,10,14]. The inverse fourth root of Oh appears to be the coefficient in Eq. (4): the smaller the Oh, the longer the inertial regime. More precisely, this regime can be observed if the inertial velocity is smaller than the viscous one, i.e., for  $\text{Oh} < 1$  which implies for a millimetric drop a viscosity typically smaller than  $100 \text{ mPa s}$ . Water obviously belongs to this category, but also many oils, most solvents and liquid metals.

- 
- [1] S. Smith, ZAMP **20**, 556 (1969).  
 [2] J. Lopez, C.A. Miller, and E. Ruckenstein, J. Colloid Interface Sci. **56**, 460 (1976).  
 [3] L.H. Tanner, J. Phys. D **12**, 1478 (1979).  
 [4] H.E. Huppert, J. Fluid Mech. **121**, 43 (1982).  
 [5] P.G. de Gennes, C. R. Acad. Sci., Ser. II: Mec., Phys., Chim., Sci. Terre Univers **298**, 111 (1984).  
 [6] P.G. de Gennes, Rev. Mod. Phys. **57**, 827 (1985).  
 [7] A.M. Cazabat and M.A. Cohen-Stuart, J. Phys. Chem. **90**, 5845 (1986).  
 [8] A. Nakajima, K. Hashimoto, and T. Watanabe, Monatsch. Chem. **132**, 31 (2001).  
 [9] J. Eggers, J.R. Lister, and H.A. Stone, J. Fluid Mech. **401**, 293 (1999).  
 [10] L. Duchemin, J. Eggers, and C. Josserand, e-print physics/0212075.  
 [11] C. Clanet and D. Quéré, J. Fluid Mech. **460**, 131 (2002).  
 [12] D. Quéré, Europhys. Lett. **39**, 533 (1997).  
 [13] Lord Rayleigh, Proc. R. Soc. Edinburgh **29**, 71 (1879).  
 [14] P. Kavehpour, B. Ovrnyn, and G.H. McKinley, Colloids Surf., A **206**, 409 (2002).